HHS Public Access

Author manuscript

Gene Ther. Author manuscript; available in PMC 2022 April 07.

Engineered AAV8 capsid acquires heparin and AVB sepharose binding capacity but has altered *in vivo* transduction efficiency

Laura P. van Lieshout[1], **Ashley A. Stegelmeier**[1], **Tara N. Rindler**[2,3], **John J. Lawder**[4], **Debra L. Sorensen**[5], **Kathy L. Frost**[5], **Stephanie A. Booth**[5,6], **James P. Bridges**[7], **Sarah K. Wootton**[1,*]

[1]Department of Pathobiology, University of Guelph, Guelph, Ontario, Canada

[2]Department of Pediatrics, University of Cincinnati, College of Medicine, Cincinnati, OH USA

[3]Division of Pulmonary Biology, Cincinnati Children's Hospital Medical Center, Cincinnati, OH USA

[4]Department of Molecular Genetics, Biochemistry, and Microbiology, University of Cincinnati, College of Medicine, Cincinnati, OH

[5]Molecular Pathobiology, National Microbiology Laboratory NML, Public Health Agency of Canada, Winnipeg, Manitoba, Canada

[6]Department of Medical Microbiology and Infectious Diseases, University of Manitoba, Winnipeg, Manitoba, Canada

[7]Division of Pulmonary, Critical Care and Sleep Medicine, National Jewish Health, Denver Colorado, USA

Abstract

Naturally occurring adeno-associated virus (AAV) serotypes that bind to ligands such as AVB sepharose or heparin can be purified by affinity chromatography, which is a more efficient and scalable method than gradient ultracentrifugation. Wild type AAV8 does not bind effectively to either of these molecules, which constitutes a barrier to using this vector when a high throughput design is required. Previously, AAV8 was engineered to contain a SPAKFA amino acid sequence to facilitate purification using AVB sepharose resin; however, *in vivo* studies were not conducted to examine whether these capsid mutations altered the transduction profile. To address this gap in knowledge, a mutant AAV8 capsid was engineered to bind to AVB sepharose and heparan sulfate (AAV8-AVB-HS), which efficiently bound to both affinity columns, resulting in elution yields of >80% of the total vector loaded compared to <5% for wild type AAV8. However, *in vivo* comparison by intramuscular, intravenous, and intraperitoneal vector administration demonstrated a significant decrease in AAV8-AVB-HS transduction efficiency without alteration of the transduction profile. Therefore, although it is possible to engineer AAV capsids to bind various

*Correspondence should be addressed to: S.K.W: kwootton@uoguelph.ca.

Conflict of Interest

The authors declare no conflicts of interest.

affinity ligands, the consequences associated with mutating surface exposed residues have the potential to negatively impact other vector characteristics including *in vivo* potency and production yield. This study demonstrates the importance of evaluating all aspects of vector performance when engineering AAV capsids.

Introduction

Adeno-associated virus (AAV) vectors offer an efficient means of *in vivo* gene transfer and have established a strong record of clinical safety over the past two decades (1–3). AAV based gene therapies for dozens of genetic disorders have made significant progress in clinical trials recently (4–6), exhibited by the United States Food and Drug Administration's approval of Luxturna to treat inherited retinal disease (7) and Zolgensma to treat spinal muscular atrophy in paediatric patients (8). One of the major drawbacks of AAV based therapies is the cost associated with manufacturing large quantities of vector under good manufacturing practices (GMP) conditions, in part due to a production bottleneck caused by the lack of scalable purification methods. Indeed, Glybera was considered the most expensive drug in the world (9) and has been removed from the market over cost drawbacks, despite its demonstrated effectiveness at curing lipoprotein lipase deficiency. More cost-effective production methods are required for promising gene therapies to be translated from bench to bedside to treat a wide range of monogenic diseases. Ultracentrifugation using cesium chloride or iodixanol gradients is the standard purification method for research grade AAV; however, this approach does not scale efficiently for large crude lysate volumes. Affinity chromatography is more suited to purifying AAV from large volumes (10). However, while some AAV serotypes naturally bind affinity epitopes, others including AAV8 require alteration of surface exposed residues to facilitate binding.

AAV2, AAV6, and AAV-DJ capsids contain a heparan sulfate-binding motif (11–13), which serves as a cellular attachment factor during infection, and can therefore be purified using a heparin affinity column chromatography. Alternatively, AAV3B and AAV5 have a strong affinity to AVB sepharose, an affinity resin developed from single chain antibodies derived from llamas with pre-existing immunity to AAV (14). The epitope responsible for conferring AVB binding in AAV3B was demonstrated to be the SPAKFA amino acid sequence located at residues 665–670 (14). Substitution of corresponding regions of other capsids with a SPAKFA sequence conferred drastic AVB binding ability to originally poor binders such as AAV8, increasing the vector recovery in the elution fraction from 30% to 93% (14). Additionally, mutation of one residue, K333T, located in an ancillary AVB binding epitope at residues 328–333 was hypothesized to strengthen AVB binding (WO2017100704A1). However, *in vivo* experiments were not conducted in these studies, so it remained unclear if engineered AAV-SPAKFA vectors have altered transduction profiles.

AAV6 uniquely encodes a lysine at position 531 which is known to be a heparin binder (15). The AAV6-K531E mutant is almost completely devoid of heparin binding activity (16), suggesting this single residue is responsible for this interaction. The wild type AAV8 capsid contains a negatively charged glutamic acid at residue 533 (12), which when exchanged for a positively charged lysine, confers heparan sulfate binding activity (15). AAV8-E533K was

reported to increase retinal transduction compared to AAV8 following intravitreal injection, which was attributed to an uptake in vector accumulation within the retina (17, 18).

AAV8 is becoming more popular in the clinic because there is less pre-existing immunity to this serotype compared to other capsids such as AAV2 (19). However, AAV8 does not bind to either AVB sepharose or heparan sulfate, reducing the potential affinity ligands that can be selected for purification. The introduction of affinity binding motifs to devoid AAV capsids facilitates purification by more efficient and scalable methods, which in turn reduces the cost to manufacture these vectors. As such, we sought to engineer an AAV8 mutant capable of binding to both AVB sepharose and heparin ligands (AAV8-AVB-HS) to determine whether efficient purification could be achieved in this manner. Moreover, AAV8 and AAV8-AVB-HS transduction profiles were evaluated *in vivo* by four routes of administration to elucidate alterations in vector efficiency due to the mutated residues.

Materials & Methods

Ethics.

All animal experiments were approved by the institutional Animal Care Committees at the University of Guelph, the Cincinnati Children's Hospital Medical Center, and the National Microbiology Laboratory, in accordance with the Canadian Council on Animal Care guidelines (AUPP 3827). Six to eight-week-old female BALB/c mice were purchased from Charles River Laboratories (St. Constant, Quebec, Canada) and allowed to acclimatize one week prior to experimentation. All mice were healthy and criteria was established prior to ordering mice. Mice were of the same age, sex, and shipment. Thus, no further randomization was conducted aside from randomly selecting one cage per experimental group. The investigator was not blinded during the experiment as this study was analyzing expression as quantified objectively by a machine, and not subjective parameters such as survival endpoint in a disease model.

AAV vector production for in vivo studies.

AAV8-AVB-HS was constructed by engineering the following mutations (AAV8 VP1 numbering): E533K to confer heparin sulfate binding, substitution of residues 665–670 from NQSKLN to SPAFKA to confer AVB sepharose binding, and K333T to stabilize and enhance AVB binding. An AAV vector genome expressing firefly luciferase under the control of a CASI promoter (20, 21) and the posttranscriptional regulatory element WPRE to improve transgene expression was packaged with AAV8 and AAV8-AVB-HS capsids. Both vectors were produced by the University of Pennsylvania Vector Core (22) and were purified using gradient ultracentrifugation.

AAV Vector Genome Titration—Vector samples were treated with RQ1 DNase (Promega, −20°C storage, Cat no. PR-M6101) at 37°C for 30 minutes to remove non-encapsidated DNA followed by a 75°C incubation to deactivate the enzyme. Samples were then treated with proteinase K (Invitrogen, 20mg/mL, Cat no. 17916) at 55°C for 30 minutes to degrade the capsid followed by a 10-minute incubation at 95°C to deactivate the enzyme.

Viral genomic DNA was extracted using phenol chloroform and the titers of both vectors were quantified using a Taqman qPCR assay with a linearized plasmid standard curve (23).

AAV transduction luciferase assay.

Human embryonic kidney 293T (HEK293T; CRL-3216) and HeLa cells (CCL-2) were maintained in Dulbecco's modified Eagle's medium (DMEM; Hyclone Laboratories Inc., Utah, USA) supplemented with 7% fetal bovine serum, 2 mM L-glutamine, 100 μg/ml streptomycin, and 100 units/ml penicillin in a humidified 37°C 5% CO_2 incubator. 1×10^5 cells per well were plated in 24 well dishes (Greiner Cellstar, Kremsmünster, Austria) and allowed to adhere overnight. The next day, cells were transduced at a multiplicity of infection (MOI) of 2 000 or 10 000 vg/ cell. 72 hours post transduction, monolayers were gently washed twice with cold PBS and lysed in passive lysis buffer (Promega, Wisconsin, USA) for 15 minutes. Cell lysate was used in a luciferase assay according to manufacture instructions (Promega Dual Luciferase Assay System). All cell lines were tested for mycoplasma contamination and were uncontaminated at the time of each experiment. The cell lines were not authenticated by STR profiling immediately prior to each experiment, however they were propagated from a freshly thawed vial of low passage cells from ATCC and exhibited expected morphology.

AAV administration *in vivo*.

A standardized dose of 1×10^{11} vg was delivered to each mouse using four routes of administration: intravenous (IV), intramuscular (IM), intraperitoneal (IP), or intranasal (IN). Mice were warmed under a heat lamp and restrained in a tail vein injection device to administer IV injections. Vectors were diluted in PBS to 100 μl and injected with a 29-gauge needle (BD Biosciences, California, USA). To administer IM injections, mice were restrained in a 50 mL tube with the end removed. Fur was shaved around the gastrocnemius muscle and vectors were injected in a 40 μl volume using a 27-gauge tuberculin syringe. Mice were restrained by the scruff and injected IP with a 100 μl dose in the intraperitoneal cavity using a 27-gague tuberculin syringe. Mice were lightly anesthetized with isoflurane for IN administration and restrained as previously described (24). The vector was diluted in PBS to 80 μl and delivered in two rounds of administration (40 μl each) separated by a recovery period of 20 minutes.

Luciferase *in vivo* imaging.

D-luciferin was administered IP regardless of AAV administration route 20 minutes prior to imaging using an IVIS Spectrum CT instrument (Perkin Elmer, Waltham, MA). Bioluminesence data was analyzed using Living Image software (Perkin Elmer, Waltham, MA). Luciferase expression was quantified at 7, 14, and 28 days post vector delivery.

AVB sepharose and heparin binding.

Vector AVB sepharose binding profiles were investigated using a previously described protocol (14). Briefly, 35 mL of 0.22 μm filtered crude AAV8 or AAV8-AVB-HS lysate was loaded onto a 5 mL HiTrap AVB Sepharose HP, pre-equilibrated with basal DMEM using a peristaltic pump at a flow rate of 1 mL/ minute. The column was washed first with 20 mL of

PBS, followed by 10 mL AVB.C buffer (Tris pH 7.5, 1M NaCl) and eluted with 10 mL of AVB.B buffer (20 mmol/l sodium citrate, pH 2.5, 0.4 mol/l NaCl) into 1 mL of 1 M tris pH 10 to neutralize the acidity of the elution buffer. The heparin binding profile was evaluated as previously described with minor modifications (25). Briefly, 10 mL crude AAV8 or AAV8-AVB-HS lysate was loaded onto a 1 mL HiTrap Heparin HP column (GE) that had been pre-equilibrated with basal DMEM. The column was washed with 10 mL of HBSS with $Mg^{2+}Ca^{2+}$ (HyClone) and eluted with 5 mL of HBSS with $Mg^{2+}Ca^{2+}$ supplemented with 400 mM NaCl. Samples (40 μl) from all fractions were collected for viral DNA extraction and quantification by qPCR as described above.

Small scale AAV production.

4×10^6 HEK293 cells were seeded on 10 cm plates (Corning Life Sciences, New York, USA) and allowed to adhere overnight. Four independent production replicates were completed. For each replicate, the supernatant and cell lysate were pooled from two plates at 72 hours post transfection. Supernatant was harvested directly into 15 mL tubes and cell lysate was harvested in 5 mL of cell lysis buffer (150 mM NaCl, 50 mM Tris-HCl pH 8.5). Both fractions were subjected to three freeze thaw cycles and clarified by centrifugation. 40 μl samples were collected from each fraction and viral DNA was extracted and quantified by qPCR as described above.

Capsid Structural Modelling—The Protein Data Bank file 6V12 was used to generate a model of AAV8 capsid surface. Images were generated using the Pymol program (https://pymol.org).

Statistical Analysis—Four mice were used per experimental group, and graphs contain the individual data points for each mouse. Four independent production replicates were used for all experiments analyzing affinity binding profiles. Each experiment with 4 biological replicates per group was conducted once. Sample size was selected based on a single cage housing 4 mice.

GraphPad Prism v.7 software (GraphPad, California, USA) was used to generate all graphs and for statistical analyses. Error bars in all graphs represent standard deviation of the mean. Two-way ANOVA tests were used to determine statistical significance between each AAV vector construct and at each time point. Adjustments were not made for multiple comparisons. Graphs contain the following p value annotations: *$p<0.05$, **$p<0.01$, ***$p<0.001$, ns = not significant. Centre values reported throughout the manuscript are the mean. The data meet the assumption of the test. As estimate of variation as not provided within each group of data. No data was excluded as an outlier.

Results

AAV8-AVB-HS can be successfully purified using AVB sepharose and heparin affinity chromatography

The heparin binding mutation (E533K) and the AVB binding mutations (NQSKLN to SPAKFA substitution at residues 665–670, K333T) introduced in the AAV8 capsid to

generate AAV8-AVB-HS allowed the vector to be successfully purified from both heparin and AVB sepharose resins. After purification using a heparin column, 90.4% of the total AAV8-AVB-HS loaded was detected in the elution step (Table 1; Fig. 1A, 1B), in comparison to AAV8, which did not efficiently bind to the heparin column with 59.9% of the vector contained within the flow through and only 13.4% in the elution. Additionally, AAV8-AVB-HS was also able to be purified on an AVB sepharose column, as evidenced by 81.2% of the vector observed in the elution fraction compared to a negligible 0.2% of wildtype AAV8. Evidently, engineering the AAV8 capsid to bind AVB sepharose and heparin resulted in vector that could be efficiently purified by two methods of affinity chromatography.

Production yield and *in vitro* transduction efficiency of AAV8-AVB-HS is reduced

AAV8 is naturally a poor transducer of cells *in vitro*; however, AAV8-AVB-HS transduced HeLa and HEK 293T cells 13- and 3-fold less efficiently, respectively, than the wild type vector at a MOI of 10 000 (Fig. 1C, 1D). At a MOI of 2 000, a non-significant 2-fold decrease in luciferase expression was observed for both cell lines. In contrast, Wang *et al.* observed AAV8-SPAKFA marginally outperforming wild type AAV8 transduction in Huh7 cells (14), suggesting the SPAKFA domain impacts *in vitro* transduction in a cell dependant manner or that the heparin binding domain of AAV8-SPAKFA-HS is reducing transduction efficiency. However, AAV2 and AAV6 are some of the best *in vitro* transducers and both bind to heparin (11, 15, 26).

Small scale vector production assays demonstrated a significant decrease in vector yield using the AAV8-AVB-HS capsid compared to AAV8 in the total crude lysate (Fig. 1E). Further analysis quantifying the vector present in the cell pellet and the supernatant confirmed a decrease in AAV8-AVB-HS production yield in both fractions by 3.1-fold and 2.1-fold respectively (Fig. 1F). The distribution of the vector present in the cell lysate and the supernatant remained consistent but less vector was generated for AAV8-AVB-HS potentially indicating the capsid is less stable than AAV8 and therefore less efficiently able to assemble intact vectors. As such, although affinity chromatography can be used to purify AAV8-AVB-HS, the resulting decrease in both transduction efficiency and production yield constitute a barrier to large scale economical manufacturing processes.

AAV8 retains more potent transduction efficiency than AAV-AVB-HS across four routes of vector administration in mice

AAV8-AVB-HS was compared to wild type AAV8 firefly luciferase vector using an *in vivo* imaging system (IVIS) to quantify transgene expression following intranasal (IN), intramuscular (IM), intravenous (IV), and intraperitoneal (IP) injection. Groups of BALB/c mice (n=4/ group) received 1×10^{11} vg of either AAV8-luciferase or AAV8-AVB-HS-luciferase by one of four administration routes and were evaluated for 28 days post administration.

AAV8-mediated 80-, and 16-fold greater luciferase expression in the lung than AAV8-AVB-HS at 14 and 28 days post IN administration, respectively (Fig. 2A). AAV8-AVB-HS lung specific expression was just slightly above background levels. Although all AAV8 treated

mice displayed much stronger transgene expression there were two high expressers and two low expressers, indicating some variations in administration. Conversely, expression in the nose was comparable between both vectors at 28 days (Fig. 2B, 2C).

Following IM injection, both AAV8 and AAV8-AVB-HS demonstrated strong luciferase expression localized in the muscle, however the wild type vector generated 13-, 18-, and 62-fold greater transgene expression in the muscle than AAV8-AVB-HS (Fig. 3A). Our group and others have previously reported AAV8-mediated liver expression following IM injection (27–29); however, interestingly this liver expression phenotype was not observed when AAV8-AVB-HS was administered (Fig. 3B).

IV administration resulted in the greatest discrepancy between the wild type and engineered AAV8 vectors. AAV8 mediated 396- and 371-fold increased luciferase expression than AAV8-AVB-HS on days 14 and 28 post administration respectively (Fig. 4A). Despite the difference in magnitude, the transduction profile remained similar between vectors, with expression localized primary to the liver (Fig. 4B).

Similar to the IV route, IP administration resulted in similar distribution profiles between vectors, indicating the systemic tropism of AAV8-AVB-HS is not altered (Fig. 4C). However, the magnitude of AAV8-AVB-HS expression was significantly impaired compared to AAV8, with 84- and 29-fold reduced luciferase expression on days 14 and 28 post vector administration respectively (Fig. 4D).

Discussion

Advances in AAV-mediated gene therapies are generating effective treatments for a wide range of human diseases (3, 4). Clinical trials require much higher quantities of vector than preclinical research using murine models due to a more than three magnitude increase in subject weight. Therefore, methods to improve large scale vector production provide valuable research advancements to manufacturing commercially viable therapeutics. Purifying AAV8 via affinity chromatography would address pressing production issues because this method is more efficient and scalable than gradient ultracentrifugation. Previously, a SPAKFA sequence was added to AAV8 to expand its binding capabilities (14); however, *in vivo* studies were not conducted to determine the effect these mutations had on tissue tropism or transduction efficiency. These are crucial aspects of vector engineering that must be examined before vectors with mutated binding capabilities can be widely adopted. Here, we demonstrate that successful mutation of AAV8 to bind heparin and AVB sepharose resins also results in a decrease in transduction efficiency and *in vivo* gene product expression.

Overall, generating AAV8-AVB-HS expanded the binding capabilities of AAV8 but reduced *in vivo* transduction efficiency through four routes of administration. All mice that were administered AAV8-AVB-HS displayed decreased luciferase expression compared to AAV8 controls with the exception of comparable transgene expression in the nose following IN delivery. This indicates that AAV8-AVB-HS may be well suited for therapies that are administered via IN and are designed to target the nasal cavity. For example, intranasal

administration was used to deliver the therapeutic lysosomal enzyme α-L-iduronidase (IDUA) using AAV8 as the vector (30). In contrast, our findings demonstrate that the IM, IV, and IP routes of administration resulted in significant decreases in luciferase expression indicating the mutations that successfully conferred binding to AVB sepharose and heparin also had a deleterious effect on transduction. AAV8-AVB-HS was less efficient at transducing a variety of cell types than AAV8, and while vector yields were also lower than the wild type capsid the titers were high enough to facilitate *in vitro* and *in vivo* transduction assays. Additionally, administering AAV8-AVB-HS i.v. resulted in new expression within the bladder of the mice. A previous study using AAV8 to correct for Wilson's disease and its associated dysregulation of copper storage measured excretion in the urine of mice (31). Researchers determined that different variants of AAV8 led to differential copper excretion in the urine. Although capsid excretion was not measured in our study, it is feasible that higher transduction within the bladder could contribute to a higher turnover rate of transduced cells and excretion of the capsid, and thus a lower overall quantified total flux.

Although the concept of AAV capsid engineering to introduce an epitope binding domain is attractive for both research and clinical grade purification, the SPAKFA sequence in AAV8 resulted in lower production yields and *in vivo* transgene expression. It is possible that the SPAKFA plus the heparin binding mutation acted in negative synergism to reduce *in vivo* transduction efficiency. However, due to the fact that the location of the SPAKFA residues and the E533K mutation are on the 5-fold axis of symmetry or pore region of the capsid, it is likely these mutations had a greater influence on packaging and transduction than the heparin binding mutation located at the base on the 3-fold axis or spike region (Fig. 5). Previous studies have demonstrated that capsid mutations can alter the tropism (32) or efficiency of AAV receptor binding and thus diminishing transduction efficiency (33). Capsid mutations have also influenced the degree to which a mutant is resistant to neutralization from antibodies (34).

POROS™ CaptureSelect™ AAVX is a relatively new universal affinity binding epitope that is worth noting (35). This resin shows a very high affinity for every serotype tested so far suggesting the existence of a highly conserved epitope on AAV capsids. However, protocols are still being refined to optimize the needs of vector production and reduce the relatively high costs of these resins. While universal resins still require significant effort in downstream process development across different capsids while a specific affinity ligand interaction is more consistent across engineered capsids enabling less serotype specific development, the development of superior binding columns or resins may very well replace all other affinity chromatography methods in the future. Such an advancement in the field would allow capsid engineering to focus on other design aspects such as mitigating or evading the immune response and optimizing cell-specific transduction. Indeed, altering the column to match the viral biology instead of engineering the virus to match the column would minimize the unwanted trade-offs that were observed in this study.

Our research sets the foundation for future studies to further explore how mutating the AAV8 capsid changes transduction profiles. Neonatal mice are a key area of interest to develop gene therapies for pediatric diseases. It has been previously shown that AAV8 is superior at delivering genes to the murine brains of neonates compared to AAV-1 or −2 (36).

Indeed, administering AAV8 to neonates results in widespread distribution in the brain (37) including the dorsal root ganglion (38), albeit no microglial transduction (37). We expect that administering AAV8-AVB-HS to neonates would have a similar reduction in transduction as was observed in adult mice, although future studies are warranted to explore this area in depth. Another area of research worth exploring is the effect of mutating only AVB or HS alone to create AAV8-AVB and AAV8-HS. Within this study we included both mutations to create a vector with wide purification column tropism to be useful for a wide range of pre-existing lab workflows. It may be possible that a single mutation will have less effect on the vector tropism.

Here we have established that AAV8 can be engineered to bind both AVB sepharose and heparin allowing the AAV8-AVB-HS vector to be efficiently purified by both these affinity ligand resins. However, these combined mutations result in lower production yield as well as impaired *in vitro* and *in vivo* transduction. This study clearly demonstrates that when engineering one aspect of an AAV capsid to fit an ideal profile there can be unanticipated consequences and a comprehensive approach is required to properly evaluate engineered capsids for further development.

Acknowledgements

We thank all those involved in the care of the animals for these studies at all institutions.

Funding

Operating funds were from the Canadian Institute of Health Research (SKW - grant # 352532), the Canadian Lung Association (SKW - grant # 052919), and the National Institute of Health (JPB - HL131634). LPvL was funded by an Ontario Graduate Scholarship. AAS was funded by a Vanier Canada Graduate Scholarship, Brock Doctoral Scholarship, and the Ethel Rose Charney Scholarship in the Human/Animal Bond.

References

1. Kaplitt MG, Feigin A, Tang C, Fitzsimons HL, Mattis P, Lawlor PA, et al. Safety and tolerability of gene therapy with an adeno-associated virus (AAV) borne GAD gene for Parkinson's disease: an open label, phase I trial. The Lancet. 2007;369(9579):2097–105.
2. Kay MA, Nakai H. Looking into the safety of AAV vectors. Nature. 2003;424:251.
3. Ferreira V, Twisk J, Kwikkers K, Aronica E, Brisson D, Methot J, et al. Immune responses to intramuscular administration of alipogene tiparvovec (AAV1-LPL(S447X)) in a phase II clinical trial of lipoprotein lipase deficiency gene therapy. Hum Gene Ther. 2014;25(3):180–8. [PubMed: 24299335]
4. Nathwani AC, Tuddenham EG, Rangarajan S, Rosales C, McIntosh J, Linch DC, et al. Adenovirus-associated virus vector-mediated gene transfer in hemophilia B. N Engl J Med. 2011;365(25):2357–65. [PubMed: 22149959]
5. Mingozzi F, High KA. Immune responses to AAV in clinical trials. Curr Gene Ther. 2007;7:316–24. [PubMed: 17979678]
6. Ginn SL, Amaya AK, Alexander IE, Edelstein M, Abedi MR. Gene therapy clinical trials worldwide to 2017: An update. The Journal of Gene Medicine. 2018;20(5).
7. Smalley E. First AAV gene therapy poised for landmark approval. Nat Biotechnol. 2017;35(11):998–9. [PubMed: 29121014]
8. Hoy SM. Onasemnogene Abeparvovec: first global approval. Drugs. 2019;79:1255–62. [PubMed: 31270752]
9. Morrison C. $1-million price tag set for Glybera gene therapy. Nat Biotechnol. 2015;33(3):217–8. [PubMed: 25748892]

10. Auricchio A, O'Connor E, Hildinger M, Wilson JM. A single-step affinity column for purification of serotype-5 based adeno-associated viral vectors. Mol Ther. 2001;4(4):372–4. [PubMed: 11592841]
11. Kern A, Schmidt K, Leder C, Muller OJ, Wobus CE, Bettinger K, et al. Identification of a heparin-binding motif on adeno-associated virus type 2 capsids. Journal of Virology. 2003;77(20):11072–81.
12. Xie Q, Lerch TF, Meyer NL, Chapman MS. Structure-function analysis of receptor-binding in adeno-associated virus serotype 6 (AAV-6). Virology. 2011;420(1):10–9. [PubMed: 21917284]
13. Lerch TF, O'Donnell JK, Meyer NL, Xie Q, Taylor KA, Stagg SM, et al. Structure of AAV-DJ, a retargeted gene therapy vector: cryo-electron microscopy at 4.5 A resolution. Structure. 2012;20(8):1310–20. [PubMed: 22727812]
14. Wang Q, Lock M, Prongay AJ, Alvira MR, Petkov B, Wilson JM. Identification of an adeno-associated virus binding epitope for AVB sepharose affinity resin. Molecular Therapy - Methods & Clinical Development. 2015;2.
15. Wu Z, Asokan A, Grieger JC, Govindasamy L, Agbandje-McKenna M, Samulski RJ. Single amino acid changes can influence titer, heparin binding, and tissue tropism in different adeno-associated virus serotypes. J Virol. 2006;80(22):11393–7.
16. Srivastava A, Zhong L, Zolotukhin S, Aslanidi GV, Agbandje - McKenna M, Van Vliet KM, et al. Capsid-modified, raav3 vector compositions and uses in gene therapy of human liver cancer. US Patent. 2018: 0223312 A1.
17. Woodard K, Samulski RJ. Methods and composition for targeted gene transfer. Patent. 2018:WO2018/035213 A l.
18. Woodard KT, Liang KJ, Bennett WC, Samulski RJ. Heparan sulfate binding promotes accumulation of intravitreally delivered adeno-associated viral vectors at the retina for enhanced transduction but weakly influences tropism. J Virol. 2016;90(21):9878–88. [PubMed: 27558418]
19. Calcedo R, Wilson JM. Humoral immune response to AAV. Front Immunol. 2013;4:341. [PubMed: 24151496]
20. Xing M, Wang X, Chi Y, Zhou D. Gene therapy for colorectal cancer using adenovirus-mediated full-length antibody, cetuximab. Oncotarget. 2016;7(19):28262–72.
21. Balazs AB, Chen J, Hong CM, Rao DS, Yang L, Baltimore D. Antibody-based protection against HIV infection by vectored immunoprophylaxis. Nature. 2011;481(7379):81–4. [PubMed: 22139420]
22. Lock M, Alvira M, Vandenburghe LH, Samanta A, Toelen J, Debyser Z, et al. Rapid, simple, and versatile manufacturing of recombinant adeno-associated viral vectors at scale. Human Gene Ther. 2010;21(10).
23. Aurnhammer C, Haase M, Muether N, Hausl M, Rauschhuber C, Huber I, et al. Universal real-time PCR for the detection and quantification of adeno-associated virus serotype 2-derived inverted terminal repeat sequences. Hum Gene Ther Met. 2011;23(1):18–28.
24. Lieshout LP, Domm JM, SK. W. AAV-Mediated Gene Delivery to the Lung. Adeno-Associated Virus Vectors 2019. p. 361–72.
25. van Lieshout LP, Domm JM, Rindler TN, Frost KL, Sorensen DL, Medina SJ, et al. A novel triple-mutant AAV6 capsid induces rapid and potent transgene expression in the muscle and respiratory tract of mice. Mol Ther Methods Clin Dev. 2018;9:323–9. [PubMed: 30038936]
26. Halbert CL, Allen JM, Miller AD. Adeno-associated virus type 6 (AAV6) vectors mediate efficient transduction of airway epithelial cells in mouse lungs compared to that of AAV2 vectors. J Virol. 2001;75(14):6615–24. [PubMed: 11413329]
27. van Lieshout LP, Soule G, Sorensen D, Frost KL, He S, Tierney K, et al. Intramuscular adeno-associated virus-mediated expression of monoclonal antibodies provides 100% protection against ebola virus infection in mice. J Infect Dis. 2018;217(6):916–25. [PubMed: 29365142]
28. Greig JA, Peng H, Ohlstein J, Medina-Jaszek CA, Ahonkhai O, Mentzinger A, et al. Intramuscular injection of AAV8 in mice and macaques is associated with substantial hepatic targeting and transgene expression. PLoS One. 2014;9(11):e112268.

29. Ruzo A, Garcia M, Ribera A, Villacampa P, Haurigot V, Marco S, et al. Liver production of sulfamidase reverses peripheral and ameliorates CNS pathology in mucopolysaccharidosis IIIA mice. Mol Ther. 2012;20(2):254–66. [PubMed: 22008915]

30. Wolf DA, Hanson LR, Aronovich EL, Nan Z, Low WC, Frey WH 2nd, et al. Lysosomal enzyme can bypass the blood-brain barrier and reach the CNS following intranasal administration. Mol Genet Metab. 2012;106(1):131–4. [PubMed: 22420937]

31. Murillo O, Luqui DM, Gazquez C, Martinez-Espartosa D, Navarro-Blasco I, Monreal JI, et al. Long-term metabolic correction of Wilson's disease in a murine model by gene therapy. J Hepatol. 2016;64(2):419–26. [PubMed: 26409215]

32. Gigout L, Rebollo P, Clement N, Warrington KH Jr., Muzyczka N, Linden RM, et al. Altering AAV tropism with mosaic viral capsids. Mol Ther. 2005;11(6):856–65. [PubMed: 15922956]

33. Wu P, Xiao W, Conlon T, Hughes J, Agbandje-McKenna M, Ferkol T, et al. Mutational analysis of the adeno-associated virus type 2 (AAV2) capsid gene and construction of AAV2 vectors with altered tropism. J Virol. 2000;74(18):8635–47. [PubMed: 10954565]

34. Tseng YS, Agbandje-McKenna M. Mapping the AAV capsid host antibody response toward the development of second generation gene delivery vectors. Front Immunol. 2014;5:9. [PubMed: 24523720]

35. Nass SA, Mattingly MA, Woodcock DA, Burnham BL, Ardinger JA, Osmond SE, et al. Universal method for the purification of recombinant AAV vectors of differing serotypes. Mol Ther Methods Clin Dev. 2018;9:33–46. [PubMed: 29349097]

36. Broekman ML, Comer LA, Hyman BT, Sena-Esteves M. Adeno-associated virus vectors serotyped with AAV8 capsid are more efficient than AAV-1 or −2 serotypes for widespread gene delivery to the neonatal mouse brain. Neuroscience. 2006;138(2):501–10. [PubMed: 16414198]

37. Chakrabarty P, Rosario A, Cruz P, Siemienski Z, Ceballos-Diaz C, Crosby K, et al. Capsid serotype and timing of injection determines AAV transduction in the neonatal mice brain. PLoS One. 2013;8(6):e67680.

38. Foust KD, Poirier A, Pacak CA, Mandel RJ, Flotte TR. Neonatal intraperitoneal or intravenous injections of recombinant adeno-associated virus type 8 transduce dorsal root ganglia and lower motor neurons. Human Gene Ther. 2008;19(1).

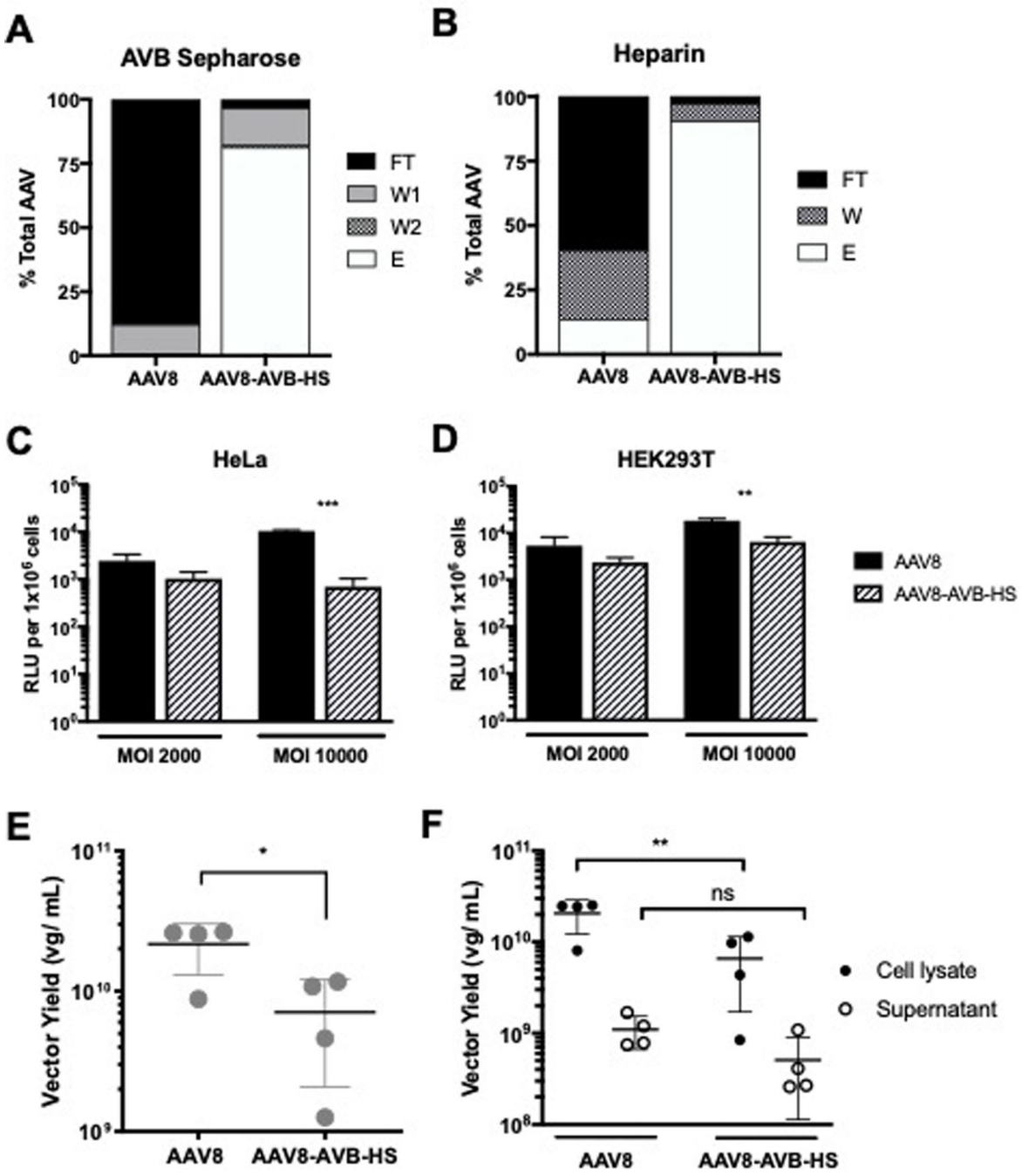

Figure 1. Affinity column binding profiles and *in vitro* characterization of AAV8 and AAV8-AVB-HS vectors.

Proportion of crude vector lysate observed in each fraction following loading onto (A) AVB sepharose or (B) heparin affinity columns (n=4). FT- flow through, W- wash, E- elution. Vector mediated luciferase expression *in vitro* in (C) HeLa and (D) HEK293T cells. Transgene expression was quantified after 72 hours and the results are shown as the background subtracted relative light units (RLU) per 1×10^6 cells (n=3). (E) Vector yield from total crude lysates 72 hours post transfection for small scale AAV production assay (n=4). (F) Vector yields in the cell lysate and supernatant fractions were quantified

separately (n=4). Error bars represent standard deviation. Statistical significance was determined with 2-way ANOVA. *p<0.05, **p<0.01, ***p<0.001, ns = not significant.

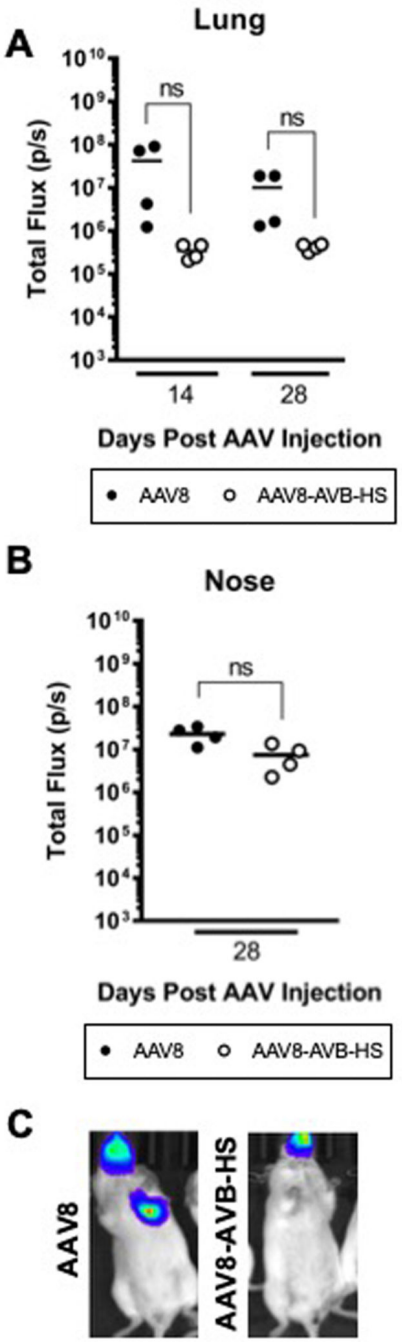

Figure 2. AAV8 and AAV8-AVB-HS transduction profile following intranasal administration.

(A) Luciferase expression generated from the lungs of mice was quantified at 7, 14 or 28-days post intranasal (IN) vector delivery and (B) expression in the nose was quantified on day 28 post vector delivery. (C) Representative images of mice that received AAV8 or AAV8-AVB-HS 14 days post vector delivery by IN administration demonstrate the distribution of transgene expression. 2-way ANOVA were used to determine statistical significance between the vectors at each time point; ns- not significant.

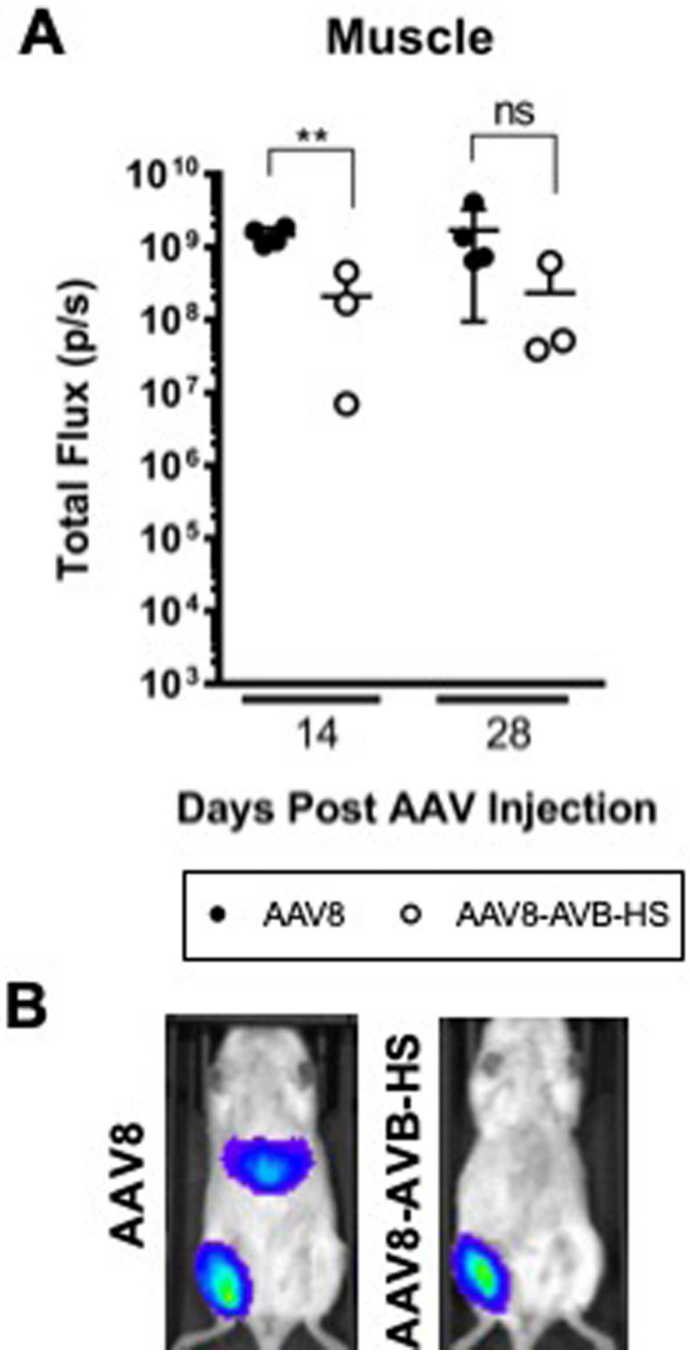

Figure 3. AAV8 and AAV8-AVB-HS transduction profile following intramuscular administration.

(A) Intramuscular luciferase expression was quantified at the site of injection at 7, 14 or 28-days post intramuscular (IM) injection excluding the abdominal signal. (B) Representative images of mice that received AAV8 or AAV8-AVB-HS 14 days post vector delivery by IM administration demonstrate the distribution of transgene expression. 2-way ANOVA were used to determine statistical significance between the vectors at each time point. *$p<0.05$, **$p<0.01$, ns-not significant.

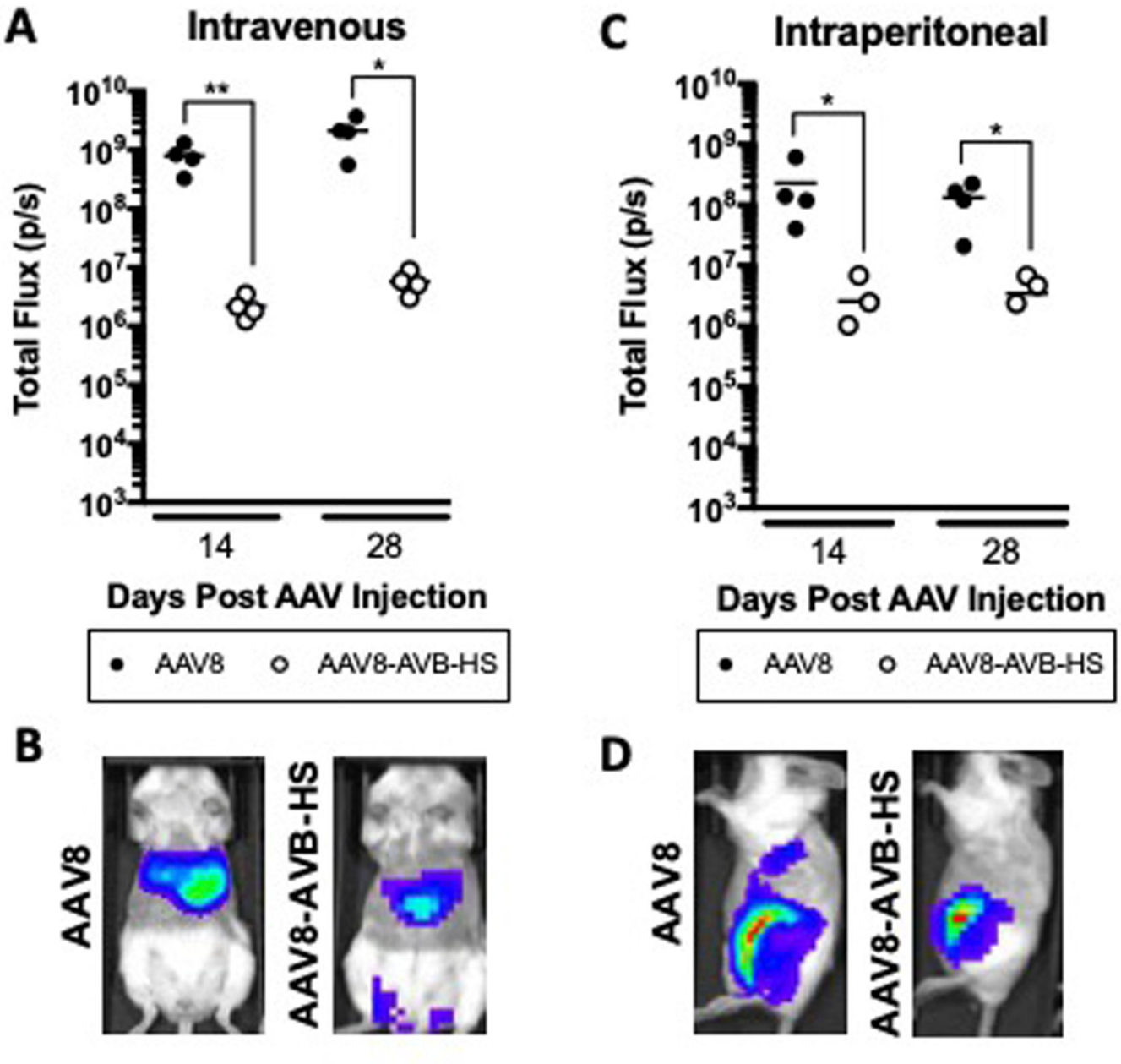

Figure 4. AAV8 and AAV8-AVB-HS transduction profile following two routes of systemic administration.

Luciferase expression generated from the abdomen was quantified at 7, 14 or 28-days post (A) intravenous (IV) and (C) intraperitoneal (IP) vector delivery. Representative images of mice that received AAV8 or AAV8-AVB-HS on day 14 post vector delivery demonstrate the distribution of transgene expression following (B) IV or (D) IP injection. 2-way ANOVA was used to determine statistical significance between the vectors at each time point. *p<0.05, **p<0.01.

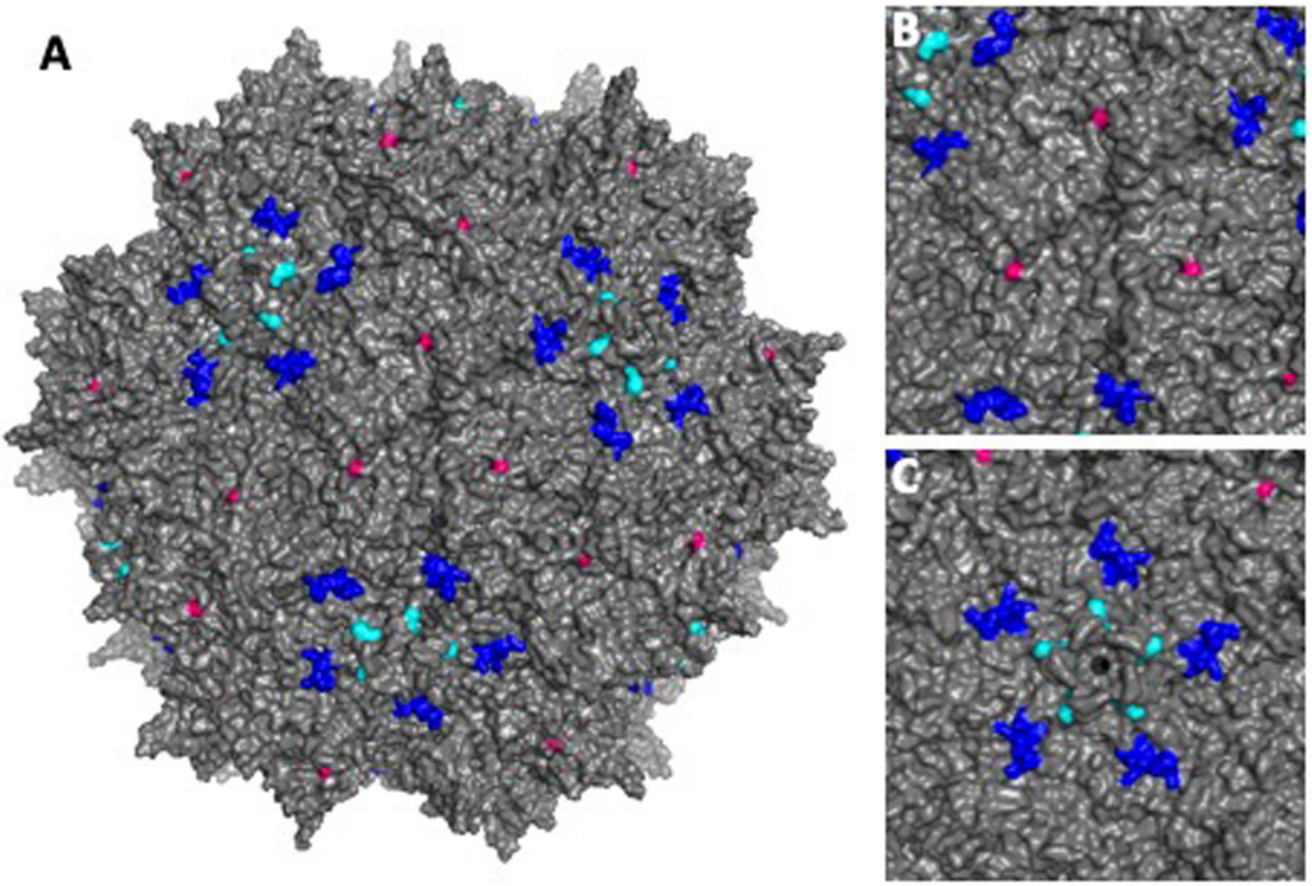

Figure 5. Structural Model of AAV8 Capsid Highlighting Mutated Binding Domains.

(A) AAV8 capsid demonstrating the location of the heparin binding mutation at residue 533 in pink, the AVB sepharose binding mutation at residues 665–670 in blue and the AVB stabilizing mutation at residue 333 in cyan. (B) View of capsid 3-fold axis of symmetry and (C) view of capsid 5-fold axis of symmetry.

Table 1:

Proportion of total crude lysate vector observed in each fraction following loading onto heparin or AVB sepharose purification columns for AAV8 and AAV8-AVB vectors

	Flow Through	Wash 1	Wash 2	Elution
Heparin				
AAV8	59.9%	26.6%	n/a	13.4%
AAV8-AVB-HS	2.8%	6.7%	n/a	90.4%
AVB Sepharose				
AAV8	87.8%	11.3%	0.5%	0.2%
AAV8-AVB-HS	3.5%	14.2%	0.9%	81.2%

n/a: not applicable